Towards field evidence for anelastic and dispersive AVF reflections

Chris Bird and Kris Innanen

ABSTRACT

Strongly anelastic seismic targets are expected to exhibit amplitude-vs.-frequency (AVF) variations. Some field and laboratory evidence of this type of behaviour exists, but much more evidence is needed before definitive statements are made about the benefit of AVF to monitoring and/or exploration. The Ross Lake heavy oil field has been subject to several VSP experiments through geological structures with strong variations in Q; one of the reflectors, at the top of the Mannville group, is a reasonable AVF candidate. By combining a time-frequency decomposition tool with a methodology for extracting raw reflection coefficients from VSP data, we show that the Mannville reflection coefficient is consistent with an AVF-rich anelastic reflector. However, our control event exhibits frequency variations on comparable scales, and so at present the identification of AVF variations is not definitive.

INTRODUCTION

Large contrasts in anelastic properties of the Earth have frequency-dependent reflection coefficients (White, 1965; Kjartansson, 1979; Chapman et al., 2006; Lines et al., 2008; Quintal et al., 2009; Ren et al., 2009; Innanen, 2011a). This represents a potentially valuable source of information with which to characterize fluid or gas bearing geophysical targets.

The dispersive amplitude-variation-with-frequency (AVF) signature in these reflections is likely subtle. Nevertheless, some field evidence of these variations has been reported (Odebeatu et al., 2006), and this evidence is further supported by a growing body of laboratory work (Lines et al., 2011). Before the presence of such data variations in hydrocarbon-relevant field data is accepted community-wide, however, we require a larger number of convincing field cases. Our purpose in this paper is to describe the methodology by which we might add to this number (or to the number of negative results), and show our initial results.

Evidence that anelastic reflections with dispersive AVF signatures are being generated above the ambient seismic noise level must come, initially, from environments with access to high levels of "ground truth", ideally in the form of instrumented wells. Vertical seismic profiling (VSP) data sets are optimal in this regard. Vertical seismic profiling (VSP) is a method of seismic data measurement in which the wave field generated by a surface source is measured by receivers at numerous depth in a borehole (Hardage, 1983; Hinds et al., 1996; Zhang, 2010). A major difference between VSP and surface seismic is that in a VSP experiment, both the upgoing and downgoing wavefields are recorded (Hardage, 1983). VSP surveys are valuable in delineating lithological, structural and stratigraphic properties of the subsurface and, of particular importance to this study, are also useful in determining physical properties of rocks such as absorption (Hardage, 1983; Zhang, 2010;

Stewart, 2001).

To produce plausible examples of dispersive AVF in VSP field data, we will require the following:

1. A field site with VSP data from a well which traverses geological structures with strong variations in Q;
2. A robust means of analyzing the local frequency dependence of an event, i.e., a tool for time-frequency decomposition of the seismic traces;
3. A means for separating the amplitude effects of transmission from those of reflection on a candidate AVF-rich event, i.e., a method for estimating the "bare" reflection coefficient;
4. A theory for determining the target Q from the AVF signature of the candidate event, which can be compared to independently derived Q estimates.

We next discuss our particular manner of fulfilling each of these requirements in turn.

1. Study area and VSP data set

The Ross Lake heavy oil field is located in the South-West of Saskatchewan and is owned and operated by Husky Energy Inc. (Zhang, 2010). See Figure 1. The reservoir is a channel sand, of Cretaceous age, in the Cantaur Formation of the Mannville group (Zhang, 2010). The Mannville group consists of sands and shales and is overlain by the carbonates of the Joli Fou formation (Zhang, 2010). Figure 2 shows a stratigraphic column.

In a collaboration between CREWES, Husky Energy, and Schlumberger Canada, a number of VSP experiments were performed, including a zero-offset VSP, using the well 11-25-13-17W3. The data were acquired using 3-component receivers and both horizontal and vertical vibrators (Zhang, 2010). The receiver spacing in the borehole was 7.5m.

Zhang (2010) performed a Q analysis of the Ross Lake VSP data using the spectral ratio method (for details of which see, e.g., Hauge, 1981). A profile of Q from this effort is shown in Figure 3. The profile suggests strong depth variability of Q.

2. A calibrated fast S-transform

To identify an AVF signature in the local spectrum of the reflection coefficient, a method of time-frequency decomposition is required. A fast S-transform (or FST) (Brown et al., 2010; Naghizadeh and Innanen, 2010), has recently been implemented with calibrated amplitudes. Testing indicates that the calibration offers high fidelity estimates of the local spectra of reflection events (Bird et al., 2010b,a). The output of the FST are "blocky" local spectra—averages over frequency bands, as opposed to pointwise spectra.

FIG. 1. Map of western Canada showing the Ross Lake heavy oil field. From Zhang (2010).

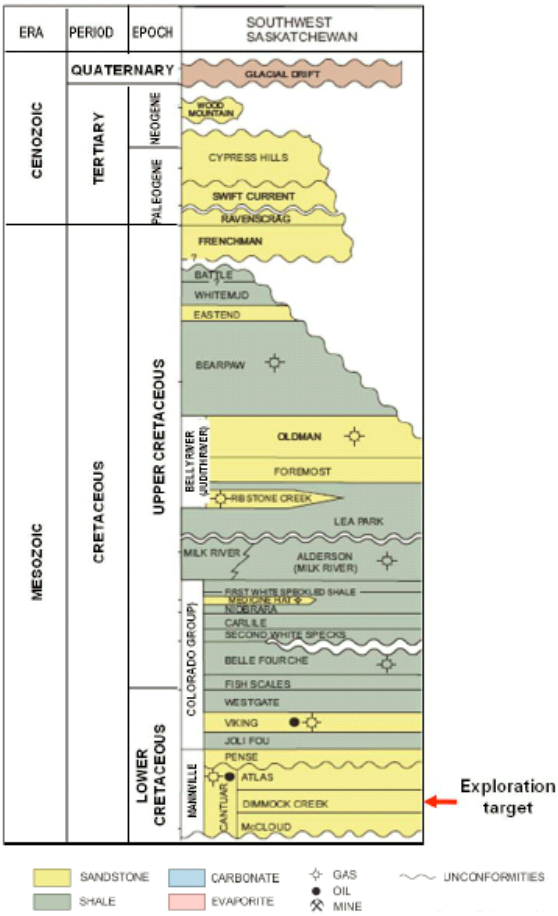

FIG. 2. Stratigraphic column of study area. From Saskatchewan Industry and Resources, 2006 adapted from Zhang (2010).

3. A method for estimation of reflection strengths from VSP data

Lira et al. (2011) have introduced a processing strategy whereby the amplitude of a reflected VSP event may be corrected to remove all transmission influences, leaving the

"bare" reflection coefficient. The method is in principle applicable in the time or the frequency domain, and hence in the presence of a suitable time-frequency decomposition is able to determine the raw spectrum of the reflection coefficient. It amounts to the division of the upgoing field by the downgoing field at or just above the reflection event.

4. AVF inversion of anelastic reflectivity

Finally, we have access to a frequency-by-frequency (AVF) method of inverting for Q from the frequency dependent absorptive reflection coefficient, developed by Innanen (2011a). This approach has been adapted for use on data in the fast S-transform domain (Bird et al., 2010b,a, 2011; Bird and Innanen, 2011) and validated extensively on synthetic data, in the presence of noise and proximal events.

A CANDIDATE REFLECTOR

Notice from Figure 3 that there is a large contrast in Q at the boundary between the Joli Fou formation and the Mannville group at 1100m depth: the quality factor in the Joli Fou carbonates is above 120 whereas Q at the top of the Mannville is below 50. Because of this contrast in Q, the primary event from the top of the Mannville is a potential example of a dispersive AVF reflection (Innanen, 2011b). We now focus on the reflection associated with this event, which we will refer to as the Mannville reflection.

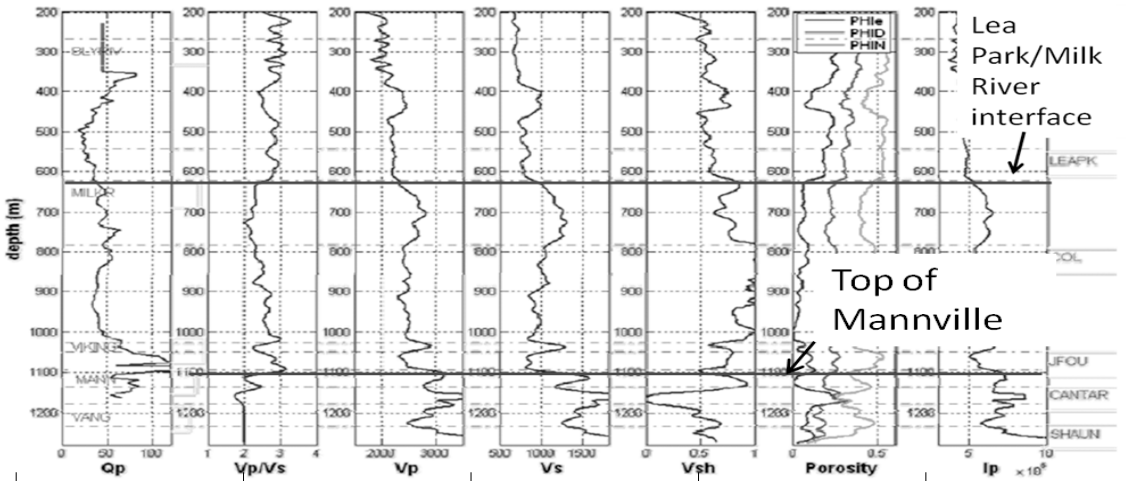

FIG. 3. Ross Lake parameter profiles. On the left-most panel is the Q profile derived using a spectral shift method. Indicated are two reflecting horizons, the top of the Mannville group and the Lea Park/Milk River interface. From Zhang (2010).

PROCESSING

Having identified a candidate reflector and its associated reflected event in the VSP data set, we must next process these data such that its "bare" reflection coefficient (i.e., the amplitude corrected for all transmission effects) is exposed as a function of frequency. This requires that we separate the direct wave from the reflected wave when they are quite close to each other, and the problem of doing this stably accounts for most of the processing issues discussed here.

We will use Lira's method twice: once, to obtain an estimate of the Mannville reflection coefficient, and once more, as a control, on a primary from the Lea Park/Milk River interface (Figures 2 and 3) in which there is very little associated contrast in Q, to compare with the Mannville reflection.

Avoidance of wave field separation

The zero-offset VSP data are plotted in Figure 4 with the two interpreted reflections. Lira's method involves forming the ratio of the reflected to the direct events as near as possible to their point of coincidence. Elsewhere (Lira et al., 2011) this has been accomplished by applying a wave field separation algorithm based on median filtering, but we did not, in this case, because the median filtering could potentially remove the AVF signature, if it exists, from the data. This means we will be forced to compare these events at shallower depths, where they are further apart.

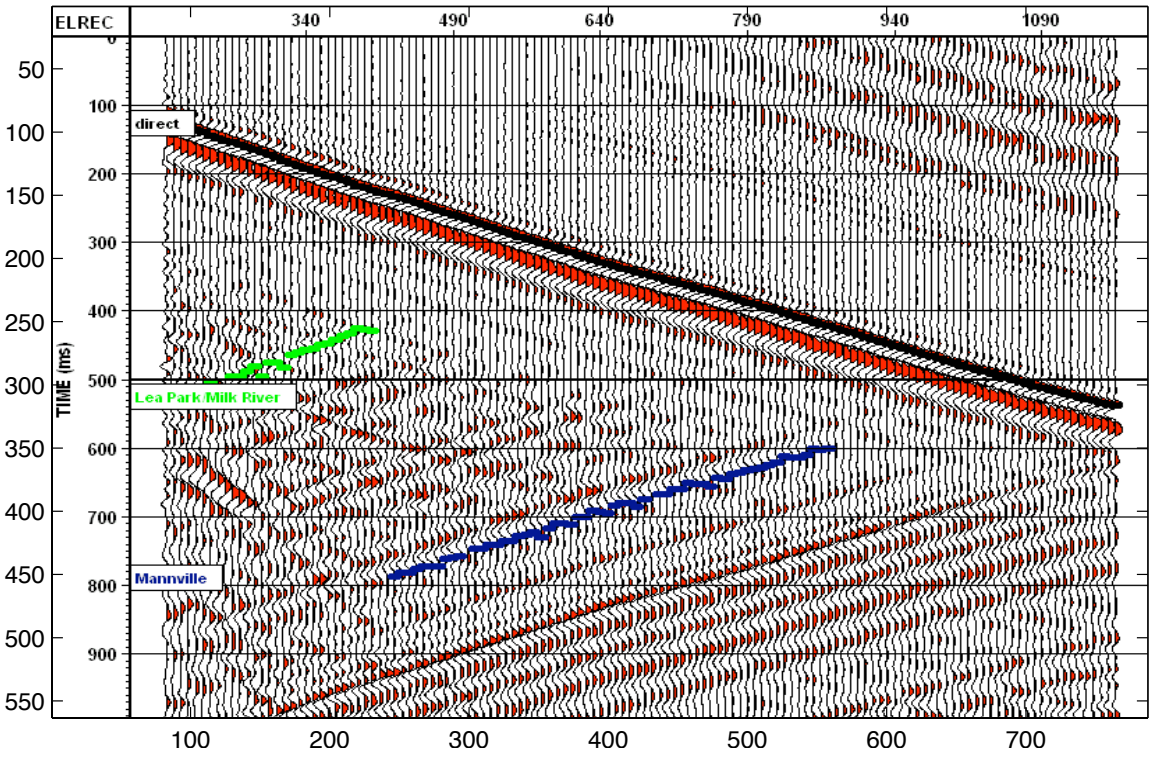

FIG. 4. VSP data from the 11-25-13-17W3 well in the Ross Lake heavy oil field. The interpreted Mannville and Lea Park/Milk river reflection events are also displayed.

Applying the FST and choosing the bandwidth

In order to provide the numerator and denominator for the division called for by Lira's method, we applied the FST to the VSP data, and extracted the spectra at the times of the interpreted events. The data used for the FST spectrum extraction were the zero-offset, stacked z-component of the full (i.e., non separated) wave field at a chosen depth. The depths of the traces used are discussed further below.

Only a portion of the bandwidth contains useable signal. The low frequency range will

be contaminated by nearby seismic events and so we must exclude the low frequencies from analysis; in our case, the exclusion was of frequencies below 31 Hz. Also, Zhang (2010) determined that the signal contains energy only up to 95 Hz so we have included the FST band 62-124 Hz but none higher.

Additional Q compensation

Since the full (un-separated) wave field was used, to distinguish between the reflection and the direct event we must use receivers which are a significant distance up the borehole from the reflector. In Figure 4 the reason is clear: the direct arrival dominates the signal so strongly that the primary is not visible until it travels up to the receiver located at 872m depth, a distance of 225m above the reflector.

This non-negligible distance can re-introduce some of the transmission effects Lira's method is designed to suppress. However, Lira et al. (2011) showed that the approximation of the reflection coefficient in an attenuative medium is given by

$$R_{est} = \frac{|P|}{|D|} = R \times \exp\left(\frac{-\omega(z_n - z_x)}{Q_{ave}c_{ave}}\right), \tag{1}$$

where R_{est} is the estimate of the true reflection coefficient, R, obtained by dividing the spectrum of the primary $|P|$ by the spectrum of the direct wave $|D|$. Hence, R_{est} is equal to the true reflection coefficient R multiplied by a factor $\exp[-\omega(z_n - z_x)/(Q_{ave}c_{ave})]$, where ω is frequency, z_n is the depth to the reflector, z_x is the depth to the receiver at which we record the primary and direct arrival, and Q_{ave} and c_{ave} are the average values for quality factor and velocity between z_n and z_x.

In our field data set the measurement of the primary is 225m above the reflector, and so we may not assume that $\exp[-\omega(z_n - z_x)/(Q_{ave}c_{ave})] \approx 1$. Instead, we use averages of Zhang's estimates of Q and c in the region between the reflector and the receiver (Zhang, 2010, as seen in Figure 3) and correct our reflection by the inverse of this quantity:

$$R_{cor} \approx \frac{R_{est}}{\exp\left(\frac{-\omega(z_n - z_x)}{Q_{ave}c_{ave}}\right)} = \frac{|P|}{|D|}\exp\frac{\omega(z_n - z_x)}{Q_{ave}c_{ave}}. \tag{2}$$

RESULTS

Following the above prescription, we:

1. Locate a depth in the VSP data set at which the Mannville reflection and the direct wave are separable;
2. Calculate the FST spectra of both of these events, and focus on the useable frequency bands;
3. Estimate the Mannville reflection coefficient $R(\omega)$ by dividing the reflected FST spectrum by the direct FST spectrum;

4. Compensate the result for attenuation on the path down and back from the receiver depth to the reflector.

In this section we examine the results, looking for supporting evidence (or otherwise) for anelastic AVF behaviour in reflections from large Q contrasts.

Preliminary positive evidence

Figure 5(a) shows the FST spectrum of the direct wave recorded at the receiver at a depth of 864m, and 5(b) shows the FST spectrum of the primary also recorded at 864m depth. The amplitudes of both the direct wave and the primary were corrected for geometrical spreading. The blue curve in Figure 5c shows the estimate of the frequency dependent reflection coefficient obtained by dividing the spectrum of the primary (panel b) by the spectrum of the direct arrival (panel a) before Q-compensation. The red curve in Figure 5c shows the estimate of the frequency dependent reflection coefficient after Q-compensation. The black vertical line in Figure 5c illustrates the cutoff below which the low frequencies are excluded due to interference from nearby events.

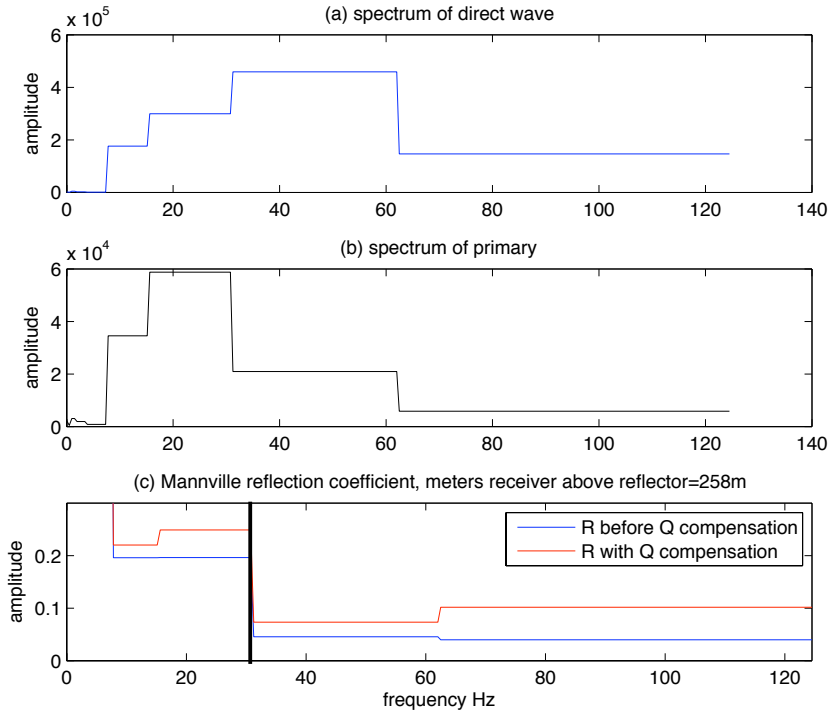

FIG. 5. Evidence of dispersive AVF reflections. (a) The spectrum of the direct arrival; (b) the spectrum of the primary reflection from the top of the Mannville formation; (c) the estimate of the reflection coefficient with Q-compensation (red) and without (blue).

Figure 5c shows that, after Q-compensation, there is an increase in the amplitude of the reflection coefficient at 62 Hz. This behaviour is consistent with standard Q models, and represents evidence that the Mannville reflector has the desired dispersive character.

Mitigating evidence

In order to evaluate whether the trend shown in Figure 5c could be an AVF signature we use Lira's method to extract an estimate of the reflection coefficient of a primary in which there is no contrast in Q. We choose then, a reflection which occurs at roughly 600m, which is interpreted as being associated with the interface between the Lea Park and Milk River Formation (see Figure 2 for the stratigraphic column). Figure 4 also shows this reflection on the VSP data, interpreted in green.

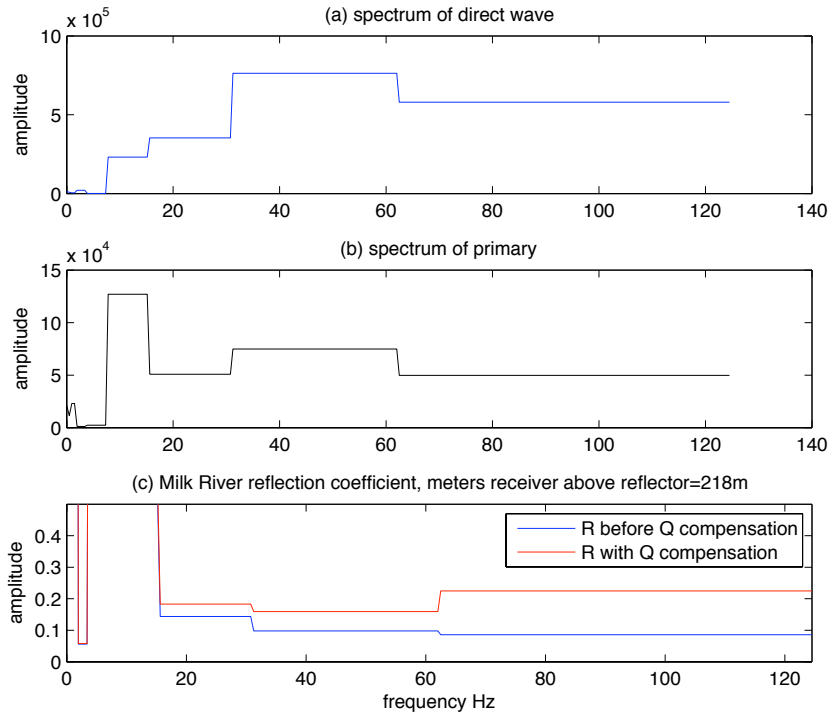

FIG. 6. (a) The spectrum of the direct arrival; (b) the spectrum of the primary reflection from the top of the Milk River formation; (c) the estimate of the reflection coefficient with Q-compensation (red) and without (blue).

Again, the signal is so dominated by the direct arrival that we do not see signal for this reflection until roughly 200m above the reflector. We apply Lira's method of estimating the frequency dependent reflection coefficient as we did for the Mannville reflection. Figure 6a shows the spectrum of the direct wave recorded by the receiver at 392m depth and and 6b shows the FST spectrum of the primary reflection from the Milk River also recorded at 392m depth. The amplitudes of both the direct wave and the primary were corrected for geometrical spreading. Figure 6c shows the spectra of the estimated reflection coefficient with the blue curve representing the estimate before Q-compensation and the red curve after Q-compensation. Again, the low frequencies are disregarded.

We see that there is an increase with amplitude of the Q-compensated reflection coefficient at roughly 62Hz in the Milk River reflector also. It is not expected that there would be an AVF signature in the reflection coefficient for this primary. Figure 7 shows the spectra for both the Milk River and Mannville primaries for comparison. The frequency

dependence of the two are of comparable orders.

Because we used average values of Q (obtained from a spectral shift method) and velocity, the frequency dependence we see in both reflection coefficients could simply be due to over-compensating the amplitudes at high frequencies. Because Q values are so low above the Milk River reflector, the Q compensation step in equation (2) may be having an unduly large influence on the results.

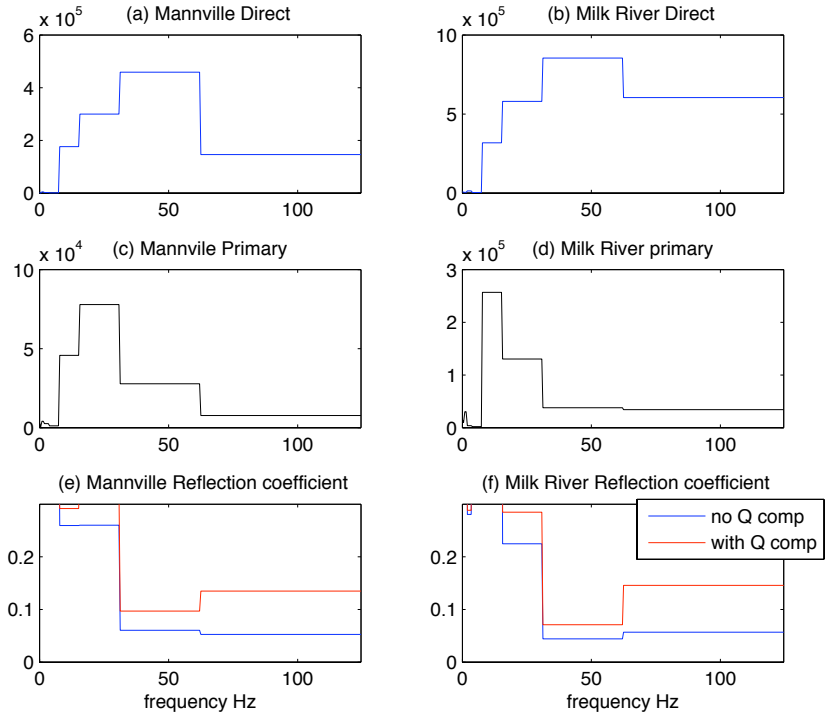

FIG. 7. Comparison of the Mannville and Milk River primaries. In (a) and (b) the spectra of the direct wave for the Mannville and Milk River formations respectively. In (c) and (d), the spectra of the primaries from the Mannville and Milk River formations and in (e) and (f), the spectra of the reflection coefficients with Q-compensation (red) and without (blue).

CONCLUSIONS

We wish to confirm or refute the presence of the theoretically predicted anelastic AVF behaviour of reflection coefficients from large Q contrasts. To do so, we applied a method developed by Lira et al. (2011), for estimating the frequency dependent reflection coefficient by comparing direct and reflected VSP events, to a zero-offset VSP data set from the 11-25-13-17W3 well in the Ross Lake Heavy oil field of South West Saskatchewan. Using the FST we obtained the spectra of both the primary and direct wave for the Mannville reflection, which a transmission analysis (Zhang, 2010) suggests is associated with a fairly large contrast in Q.

It was observed that there was an increase in the amplitude of the Mannville reflection coefficient at 62Hz, which is consistent with an AVF signature. However, in our control event, for the Milk River reflection, which is not thought to be associated with a contrast in

Q, we again find an increase in amplitude with frequency.

We suspect that the Q compensation step in the processing of the control (Milk River) event may be overcorrecting, however, since this reflector's overburden has a very low Q. Our most pressing future work will be to compare the Mannville reflection to a better control, ideally with almost infinite Q in the overburden.

We will also investigate other forms of separation of the upgoing and downgoing fields. Avoiding the Q compensation step entirely will likely add stability to our search.

When we are more satisfied with our estimate of the spectra we will also invert the spectral information to estimate the target Q. The proximity of the inverted result to the (independently derived) Q profile will be further evidence for or against the presence of the AVF signature.

ACKNOWLEDGMENTS

The sponsors of CREWES and NSERC are gratefully acknowledged for their support. We would also like to acknowledge Zimin Zhang, whose CREWES thesis research provided the Q profiles necessary for us to choose promising events.

REFERENCES

Bird, C., and Innanen, K., 2011, Full waveform inversion of anelastic reflection data: an analytic example: CREWES Sponsor's Meeting 2011, **23**, 1–5.

Bird, C., Innanen, K., Naghizadeh, M., and Lines, L., 2010a, Determination of anelastic reflectivity: how to extract seismic avf information: CREWES Annual Report, **22**, No. 4.

Bird, C., Innanen, K., Naghizadeh, M., and Lines, L., 2011, Avf inversion of anelastic reflectivity. practical issues concerning implementation.: CREWES Sponsor's Meeting 2011, **23**, 1–24.

Bird, C., Naghizadeh, M., and Innanen, K., 2010b, Amplitude calibration of a fast S-transform: CREWES Sponsor's Meeting 2010, **22**, 1–12.

Brown, R. A., Lauzon, M. L., and Frayne, R., 2010, A general description of linear time-frequency transforms and formulation of a fast, invertible transform that samples the continuous S-transform spectrum nonredundantly: IEEE Transactions on Signal Processing, **58**, No. 1, 281–290.

Chapman, M., Liu, E., and Li, X. Y., 2006, The influence of fluid-sensitive dispersion and attenuation on AVO analysis: Geophysical Journal International, **167**, No. 1, 89–105.

Hardage, B. A., 1983, Vertical Seismic Profiling, Part A: Principles, vol. 14A: Geophysical Press.

Hauge, P. S., 1981, Measurements of attenuation from vertical seismic profiles: Geophysics, **46**, No. 11, 1548–1558.
URL `http://link.aip.org/link/?GPY/46/1548/1`

Hinds, R. C., Anderson, N. L., and Kuzmiski, R. D., 1996, VSP Interpretive Processing: Theory and Practice: Society of Exploration Geophysicists.

Innanen, K. A., 2011a, Inversion of the seismic AVF/AVA signatures of highly attenuative targets: Geophysics, **76**, No. 1, R1–R11.

Innanen, K. A., 2011b, Inversion of the seismic AVF/AVA signatures of highly attenuative targets: Geophysics, **76**, No. 1, R1–R14.

Kjartansson, E., 1979, Attenuation of seismic waves in rocks and applications in energy exploration: Ph.D. thesis, Stanford University.

Lines, L., Sondergeld, C., Innanen, K. A., Wong., J., Treitel, S., and Ulrych, T. J., 2011, Experimental confirmation of "Reflections on Q": CREWES Annual Report (this report), **23**.

Lines, L. R., Vasheghani, F., and Treitel, S., 2008, Reflections on Q: CSEG Recorder, **Dec**, 36–38.

Lira, J. E., Weglein, A. B., Bird, C., and Innanen, K. A., 2011, Determination of reflection coefficients by comparison of direct and reflected vsp events: CREWES Sponsor's Meeting 2011, **23**, 1–13.

Naghizadeh, M., and Innanen, K., 2010, Fast generalized Fourier interpolation of nonstationary seismic data: CREWES Sponsor's Meeting 2010.

Odebeatu, E., Zhang, J., Chapman, M., and Li, X.-Y., 2006, Application of spectral decomposition to detection of dispersion anomalies associated with gas saturation: The Leading Edge, **February**, 206–210.

Quintal, B., Schmalholz, S. M., and Podladchikov, Y. Y., 2009, Low-frequency reflections from a thin layer with high attenuation caused by interlayer flow: Geophysics, **74**, N15–N23.

Ren, H., Goloshubin, G., and Hilterman, F. J., 2009, Poroelastic analysis of amplitude-versus-frequency variations: Geophysics, **74**, No. 6, N49–N54.

Stewart, R. R., 2001, VSP: An in-depth seismic understanding: CSEG Recorder, **September**, 79–83.

White, J. E., 1965, Reflections from lossy media: Journal of the Acoustical Society of America, **38**, 604–607.

Zhang, Z., 2010, Assessing attenuation, fractures, and anisotropy using logs, vertical seismic profile, and three-component seismic data: heavy oilfield and potash mining examples: University of Calgary.